

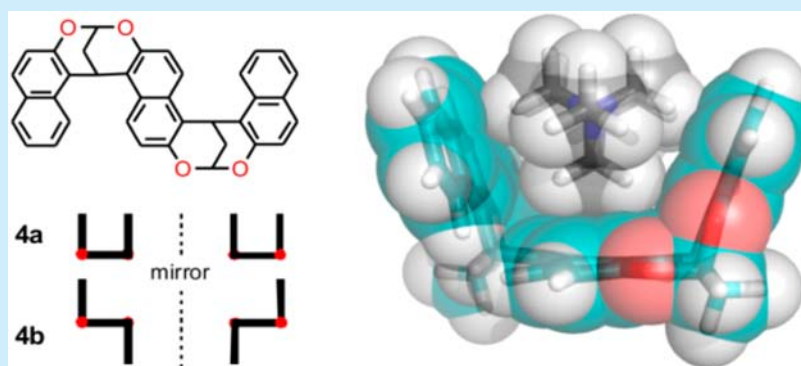
Synthesis, Solid-State Structures, and Molecular Recognition of Chiral Molecular Tweezer and Related Structures Based on a Rigid Bis-Naphthalene Cleft

Zhenfeng He,^{†,‡} Xin Yang,[†] and Wei Jiang^{*,†}

[†]Department of Chemistry, South University of Science and Technology of China, No. 1088 Xueyuan Boulevard, Nanshan District, Shenzhen, 518055, P. R. China

[‡]School of Chemical Engineering and Environment, North University of China, No. 3 Xueyuan Road, Taiyuan, Shanxi 030051, P. R. China

S Supporting Information



ABSTRACT: The rigid and nonchiral bis-naphthalene cleft was used for the first time as a scaffold to build a chiral molecular tweezer. The molecular tweezer and its related compounds have been synthesized and carefully characterized by X-ray crystallography and NMR spectroscopy. Their solid-state structures and molecular recognition properties have also been studied.

Molecular tweezers are featured by two flat, usually aromatic and identical pincers and a more or less rigid tether.¹ The tether holds the two pincers in a *syn* conformation/configuration. Their half-open cavities tend to bind flat aromatic guests.² Very rigid molecular tweezers, such as Klärner's di- to tetra-methylene-bridged molecular tweezers,³ often have good guest-binding properties, resulting in biological applications.⁴ But they usually require multistep synthesis and are not always easy to access. Chiral molecular tweezers are even rarer in literature. Two major classes are based on Tröger's base⁵ and Kagan's ether,⁶ respectively. Both of these two modules are chiral themselves. However, their synthesis and purification are often tedious. Herein, we report a new class of chiral molecular tweezer based on a nonchiral bis-naphthalene cleft. This kind of molecular tweezer is fairly easy to synthesize. Its related structures and host–guest chemistry have also been studied.

The bis-naphthalene cleft **1** (16*H*-8,16-methanodinaphtho[2,1-*d*:1',2'-*g*][1,3]dioxocin) has been known for three decades.⁷ Its well-defined curvature is ideal for creating a cavity to host guest molecules. However, its applications to supramolecular chemistry are very scarce in the supramolecular literature.^{8,9} The synthesis of **1** is actually rather straightforward: 2-naphthol and 1,1,3,3-tetramethoxypropane were stirred in the 1:2 mixture of THF and TFA at room temperature to

afford **1** in a decent yield (85%). The crystal structure of **1** was then obtained by slow evaporation of its solution in CHCl₃. As shown in Figures 1a and S1, the cleft **1** packed in a “hug from behind” fashion and forms a “supramolecular polymer” in the solid state. The neighboring molecules are in an antiparallel orientation. This results in better dipole alignments and more compact crystal packing. The crystal structure also suggests the methylene protons may have very weak C–H⋯π interactions¹⁰ (H-centroid distance: 2.79–2.89 Å) with the naphthalenes in the adjacent molecule. The dihedral angle of two naphthalenes in the same molecule is ca. 107°, defining a well-defined cleft structure¹¹ for molecular recognition. Multiple incorporation of this basic module may enable the construction of molecular tweezers.

In order to obtain a molecular tweezer, the structure of **1** has to be incorporated more than once. Relatively symmetric structures are preferable. Therefore, 2,6-dihydroxynaphthalene was used together with 2-naphthol as the basic building blocks. To test the reactivity and prepare starting materials for the synthesis of more complex structures, we thus synthesize two

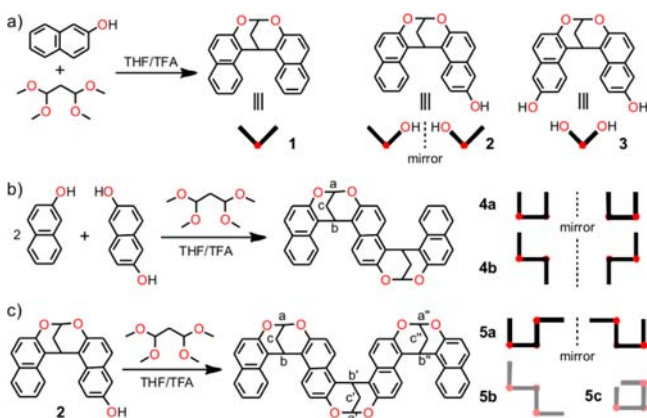
Received: June 29, 2015

Published: July 21, 2015

compounds **2** and **3** through a protection and deprotection procedure.

Analogously, the crystal structures of **2** and **3** were also obtained (Figure 1b, 1c, and S1). Surprisingly, the “hug from behind” arrangement is not observed. Instead, two clefts “dimerize” in the solid state. Again, they are arranged in an antiparallel orientation presumably to favor the dipole moment and crystal packing. Offset $\pi\cdots\pi$ stacking¹² (centroid–centroid distance: 3.54 Å for **2**; 3.64 Å for **3**) and O–H $\cdots\pi$ interactions (H–centroid distance: 2.37 Å for **2**; 2.42 Å for **3**) contribute to this dimerization. Although the cleft **1** is symmetric and nonchiral, the cleft **2** with lower symmetry is actually planar-chiral (Scheme 1). The two enantiomers of **2** are both observed

Scheme 1. (a) Modified Synthetic Procedure for Compound 1 and Chemical Structures of Its Hydroxyl Derivatives 2 and 3; (b) Synthetic Route and Structures of the Tris-naphthalene 4; (c) Synthetic Route and Structures of the Tetrakis-naphthalene 5^a



^aNumbering on the structures corresponds to the assignment of NMR signals. **5b** or **5c** are only detected by NMR and cannot be isolated in pure forms.

and they follow heterochiral self-sorting¹³ in the solid state. Introducing two hydroxyl groups does not disrupt the symmetry of **3**, and it is still nonchiral. Based on the stereochemistry of **2** and **3**, we anticipate that the tris-naphthalene **4** must be chiral, while the tetrakis-naphthalene **5** can be either chiral or achiral. Thus, we may obtain a chiral molecular tweezer from the nonchiral bis-naphthalene cleft.

The tris-naphthalene **4** can be synthesized in a one-pot procedure. However, the yield is rather low (3% for **4a**, 4% for **4b**), presumably due to the competition of many possible reaction combinations. Two tris-naphthalenes with different solubility were separated through fractional crystallization: One is more soluble in CHCl_3 , and the other is much less soluble. Their ¹H NMR spectra are shown in Figure 2. Theoretically, two isomers are possible (Scheme 1): one with two terminal naphthalenes in a *syn* configuration (**4a**); the other's terminal naphthalenes are in an *anti* configuration (**4b**). Although their NMR spectra are different (Figure 2a and 2b), they have the same peak splitting/pattern and cannot be distinguished by regular ¹H NMR. 2D NMR experiments were thus performed. All the peaks can be unambiguously assigned (Figures S2–S4), but the two still cannot be differentiated. Luckily, the single crystals of both isomers were obtained and their solid-state structures are shown in Figure 1d and 1e. The one with good solubility in CHCl_3 is proven to be **4a**, and the other one is **4b**.

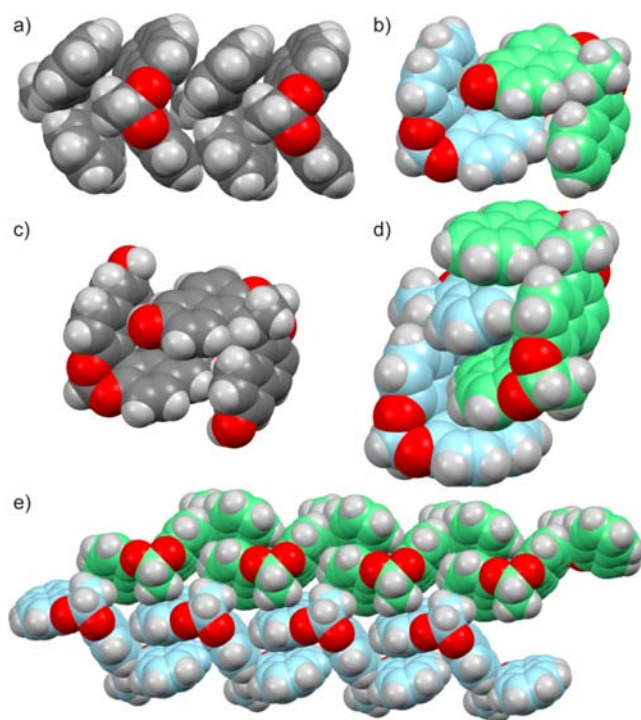


Figure 1. Single crystal structures of compounds (a) **1**, (b) **2**, (c) **3**, (d) **4a**, and (e) **4b**. For compound **2**, **4a**, or **4b**, the two enantiomers are colored in light green and light blue, respectively.

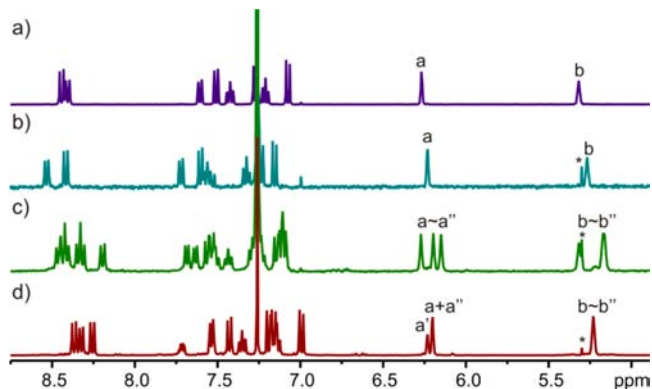


Figure 2. Partial ¹H NMR spectra (400 MHz, CDCl_3 , 25 °C) of (a) **4a**, (b) **4b**, (c) **5a**, and (d) **5b/5c**. Asterisk = residual solvent.

As discussed above, both isomers are chiral. The *syn* isomer (**4a**) “self-sorts heterochirally” in the solid state: the enantiomeric pair exists within the same “dimeric assembly”. While the *anti* isomer (**4b**) prefers homochiral self-sorting,¹⁴ each enantiomer forms a linear polymeric arrangement. Weak C–H $\cdots\pi$ interactions and offset $\pi\cdots\pi$ stacking should also be responsible for the crystal packing (Figure S1). In the present research, these enantiomers are not separated.

To further extend the cavity, we set out to synthesize the tetrakis-naphthalene **5**. Three possible isomers are expected for tetrakis-naphthalene **5** (Scheme 1): **5b** and **5c** are symmetric structures and are not chiral; **5a** has reduced symmetry and is chiral. We aimed to obtain **5c** which has a macrocycle-like cavity. The synthesis of **5** can be achieved through the dimerization of **2** under the same conditions. The yield is surprisingly low (8% for **5a**), and only one major product was isolated. After accumulation over many batches, another minor

product was obtained in a very small quantity together with some impurity (see synthetic procedures in the Supporting Information). Numerous attempts to obtain single crystal structures on the major product have been unsuccessful so far. Nevertheless, simple ^1H NMR spectra are also helpful for assigning their structures (major product, Figure 2c; minor product, Figure 2d). With respect to **5a**, three NMR peaks are expected for proton *a*, since each of the three acetal bridges are located at different environments. But for **5b** and **5c**, two peaks with 1:2 ratio are expected for protons *a*. Based on this analysis, the major product (Figure 3c) can be assigned to **5a**. 2D NMR

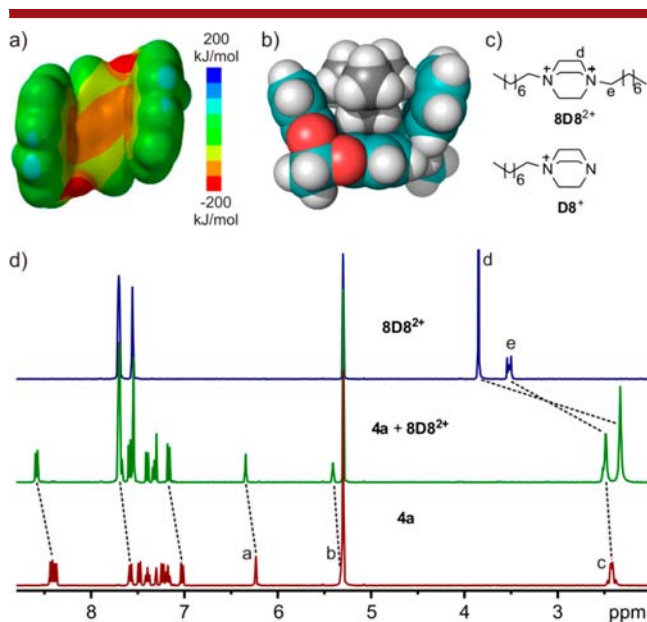


Figure 3. (a) Electrostatic potential surface of **4a** calculated at the AM1 level of theory; (b) energy-minimized structure of the complex between **4a** and a DABCO dication; (c) chemical structures of guests $8\text{D}8^{2+}$ and $\text{D}8^+$. Counterion = tetrakis[3,5-bis(trifluoromethyl)phenyl]borate anion (BArF^-); (d) Partial ^1H NMR spectra (400 MHz, CD_2Cl_2 , 2.0 mM, 25 °C) of $8\text{D}8^{2+}$, **4a**, and their equimolar mixture.

has been performed to assign almost all the peaks (Figures S5–S7). The minor product is either **5b** or **5c**. Limited by the quantity and the purity, the exact structure of the minor product is not further assigned. With either one, it suggests there is one product undetected in the product mixture. The less symmetric product **5a** is, however, favored in this reaction.

With all of these compounds in hand, we decided to test their supramolecular chemistry. Compounds **2**, **3**, and **4a** “dimerize” in the solid state. We wonder whether this is also true in solution. However, most of them have very poor solubilities. In the accessible concentration range (0.5–5.0 mM), the changes of chemical shifts are rather small to allow the determination of dimerization constants.

The calculated electrostatic potential surface (Figure 3a) suggests that the half-open cavity defined by molecular tweezer **4a** is rather electron-rich. It may well host an electron-deficient organic cation with a cylindrical or spherical shape, such as organic cations based on 1,4-diazabicyclo[2.2.2]octane (DABCO). This is supported by molecular modeling: the energy-minimized structure shows that a DABCO-based organic cation may be well accommodated by **4a** through multiple C–H $\cdots\pi$ interactions. Encouraged by this, two guests

$8\text{D}8^{2+}$ and $\text{D}8^+$ with good solubility in nonpolar solvents are selected. The noncoordinating tetrakis[3,5-bis(trifluoromethyl)phenyl]borate anion (BArF^-) is used as the counterion.¹⁵ The bis-naphthalene clefts **1** and **2**, and **4a** and **5a** were studied for their guest binding abilities. The solubility of **3** and **4b** is too poor in CD_2Cl_2 and CDCl_3 , and their binding abilities are not studied.

The binding between guest $8\text{D}8^{2+}$ and molecular tweezer **4a** was tested first. As shown in Figure 3d, significant chemical shifts on both the guest and the host were observed when mixing them in a 1:1 ratio in CD_2Cl_2 . In particular, the protons *d* on DABCO were shifted upfield by 1.38 ppm, suggesting the guest is bound inside the cavity of the tweezer and experiences the shielding effect of the naphthalenes. The methylene protons on the alkyl groups show much less upfield shifts (Figure S8), indicating that the host binds on the DABCO site, not on the alkyl groups of the guest. Free guest and free host species are not detected. Further experiments support a fast exchange complex at the NMR time scale. The ESI mass spectrum of the equimolar mixture of $8\text{D}8^{2+}$ and **4a** was then obtained (Figure S11). The base peak at m/z 1721.60 can be assigned to $[\text{8D}8\text{-BArF@4a}]^+$, suggesting a 1:1 binding stoichiometry. This is confirmed by Job’s plot (Figure 4a). Similar NMR spectra and binding stoichiometry were observed for the other complexes (Figures S12–S17).

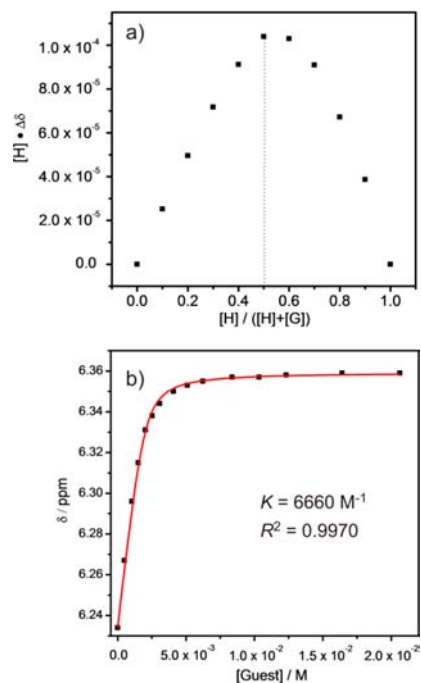


Figure 4. (a) Job’s plot for the complex between **4a** and $8\text{D}8^{2+}$ as determined by ^1H NMR experiments ($[\text{4a}] + [\text{8D}8^{2+}] = 2.0$ mM). (b) Nonlinear fitting of the NMR titration curve of **4a** by $8\text{D}8^{2+}$. The chemical shift of proton *a* on **4a** is monitored.

NMR titrations and nonlinear fitting were then performed to obtain the binding constants (Figures 4b and S18–S23). All the curves are fitted very well according to a 1:1 stoichiometry. The binding constants are listed in Table 1. Surprisingly, the bis-naphthalene clefts **1** and **2** are able to complex with guest $8\text{D}8^{2+}$. **2** is slightly better than **1**, which may be due to an additional electron-donating contribution from the hydroxyl group. The binding constant between **4a** and $8\text{D}8^{2+}$ is the

Table 1. . Binding Constants (M^{-1}) as Determined by 1H NMR Titration (400 MHz, CD_2Cl_2 , 25 °C)^a

	1	2	4a	5a
8D8 ²⁺	50 ± 3	61 ± 2	6660 ± 820	258 ± 7
D8 ⁺	– ^b	– ^b	187 ± 4	30 ± 1

^aThe concentrations of the hosts are fixed at 2.0 mM ^bThe binding constants are too small ($<10 M^{-1}$) to be accurately determined.

largest: 6660 M^{-1} , which is 100 times stronger than those of the bis-naphthalene clefts. However, the guest D8⁺ with only one charge shows much lower affinity to 4a than 8D8²⁺ does. This indicates cation $\cdots\pi$ interactions¹⁶ play an important role in the complex 8D8²⁺@4a. Indeed, neutral molecules, such as naphthalene, adamantane, and DABCO, are no guests for 4a. 5a contains the structural element of 4a and is thus expected to have a similar guest binding affinity as 4a. Surprisingly, 5a gives a much lower binding affinity. The detailed reason is still unclear. But the molecular model (Figure S24) suggests that this may be due to a disrupted cooperative binding: for 5a, the guest forms a strong C–H \cdots O hydrogen bond (2.3 Å) with the additional acetal O atom in 5a, causing the drastic change of the binding mode; this disrupts the multiple and cooperative C–H $\cdots\pi$ interactions as observed for 4a (Figure 3b), arguably resulting in a lower binding affinity.

In summary, we reported the synthesis of a new class of molecular tweezer and its related compounds based on a bis-naphthalene cleft. Although the scaffold used is not chiral, the resulting tris-naphthalene tweezer is chiral. The molecular tweezer and its related compounds have been characterized by X-ray crystallography and NMR spectroscopy. In addition, these rigid and electron-rich structures can host DABCO-based organic cations. The molecular tweezer in the present research further enriches the toolbox of supramolecular chemistry.

■ ASSOCIATED CONTENT

📄 Supporting Information

Experimental section, ESI mass spectra, 1D and 2D 1H NMR spectra, X-ray single crystal structures, and binding constant fitting curve. The Supporting Information is available free of charge on the ACS Publications website at DOI: 10.1021/acs.orglett.5b01871.

■ AUTHOR INFORMATION

Corresponding Author

*E-mail: jiangw@sustc.edu.cn.

Notes

The authors declare no competing financial interest.

■ ACKNOWLEDGMENTS

This research is financially supported by the National Natural Science Foundation of China (No. 21302090), Thousand Talents Program-Youth, and South University of Science and Technology of China (SUSTC). Prof. Tao Wang (Peking University, Shenzhen Graduate School) is acknowledged for help on solving single-crystal structures.

■ REFERENCES

- (1) Chen, C.-W.; Whitlock, H. W. *J. Am. Chem. Soc.* **1978**, *100*, 4921–4922.
- (2) (a) Hardouin-Lerouge, M.; Hudhomme, P.; Sallé, M. *Chem. Soc. Rev.* **2011**, *40*, 30–43. (b) Rowan, A. E.; Elemans, J. A. A. W.; Nolte,

R. J. M. *Acc. Chem. Res.* **1999**, *32*, 995–1006. (c) Zimmerman, S. C. *Top. Curr. Chem.* **1993**, *165*, 71–102.

- (3) Klärner, F.-G.; Kahlert, B. *Acc. Chem. Res.* **2003**, *36*, 919–932.
- (4) Klärner, F.-G.; Schrader, T. *Acc. Chem. Res.* **2013**, *46*, 967–978.
- (5) Dolenský, B.; Havlík, M.; Král, V. *Chem. Soc. Rev.* **2012**, *41*, 3839–3858.
- (6) Harmata, M. *Acc. Chem. Res.* **2004**, *37*, 862–873.
- (7) Van Allan, J. A.; Giannini, D. D.; Whitesides, T. H. *J. Org. Chem.* **1982**, *47*, 820–823.
- (8) (a) Shorthill, B. J.; Avetta, C. T.; Glass, T. E. *J. Am. Chem. Soc.* **2004**, *126*, 12732–12733. (b) Avetta, C. T.; Shorthill, B. J.; Ren, C.; Glass, T. E. *J. Org. Chem.* **2012**, *77*, 851–857.
- (9) (a) He, Z.; Ye, G.; Jiang, W. *Chem. - Eur. J.* **2015**, *21*, 3005–3012. (b) Huang, G.-B.; Jiang, W. *Prog. Chem.* **2015**, *27*, 744–754.
- (10) Nishio, M.; Hirota, M.; Umezawa, Y. *The CH/ π Interaction: Evidence, Nature, and Consequences*; Wiley-VCH: 1998.
- (11) Rebek, J., Jr.; Askew, B.; Islam, N.; Killoran, M.; Nemeth, D.; Wolak, R. *J. Am. Chem. Soc.* **1985**, *107*, 6736–6738.
- (12) Hunter, C. A.; Sanders, J. K. M. *J. Am. Chem. Soc.* **1990**, *112*, 5525–5534.
- (13) (a) Rang, A.; Nieger, M.; Engeser, M.; Lützen, A.; Schalley, C. A. *Chem. Commun.* **2008**, 4789–4791. (b) He, Z.; Jiang, W.; Schalley, C. A. *Chem. Soc. Rev.* **2015**, *44*, 779–789.
- (14) Hutin, M.; Cramer, C. J.; Gagliardi, L.; Shahi, A. R. M.; Bernardinelli, G.; Cerny, R.; Nitschke, J. R. *J. Am. Chem. Soc.* **2007**, *129*, 8774–8780.
- (15) (a) Li, C.; Shu, X.; Li, J.; Fan, J.; Chen, Z.; Weng, L.; Jia, X. *Org. Lett.* **2012**, *14*, 4126–4129. (b) Chen, H.; Fan, J.; Hu, X.; Ma, J.; Wang, S.; Li, J.; Yu, Y.; Jia, X.; Li, C. *Chem. Sci.* **2015**, *6*, 197–202.
- (16) Dougherty, D. A. *Acc. Chem. Res.* **2013**, *46*, 885–893.